# Mid-infrared laser spectroscopic determination of isotope ratios of N2O at trace levels using wavelength modulation and balanced path length detection

H. WAECHTER
M.W. SIGRIST[✉]

# Mid-infrared laser spectroscopic determination of isotope ratios of $N_2O$ at trace levels using wavelength modulation and balanced path length detection

ETH Zurich, Institute of Quantum Electronics, Laser Spectroscopy and Sensing Laboratory,
Schafmattstrasse 16, 8093 Zurich, Switzerland

**ABSTRACT** We present a new mid-infrared laser spectrometer for high-precision measurements of isotopic ratios of molecules at ppm concentrations. Results are discussed for nitrous oxide ($N_2O$), where a precision of 3‰ for a single measurement and a reproducibility of 6‰ have been achieved for a concentration of 825 ppm. The room-temperature laser source employed is based on difference-frequency generation delivering a continuous-wave power up to 23 μW at wavelengths between 4.3 μm and 4.7 μm and a line width of 1 MHz. Two different measurement methods are compared; wavelength modulation with first-harmonic detection and direct absorption spectroscopy by recording the spectrum with a data-acquisition card. Two different detection schemes were employed; either all isotopomers were measured using the long path (36 m) of the multipass cell or a balanced path length detection scheme was used, where the main isotope was measured with a beam along a shorter path (40 cm) in the multipass cell. A single-pass reference cell was designed, offering two different path lengths for balanced path length detection. All combinations of measurement methods and detection schemes were tested regarding precision of a single measurement and long-term stability. The advantages and disadvantages of various measurement approaches are discussed.

**PACS** 42.62.Fi; 42.65.Ky; 32.10.Bi

## 1 Introduction

Trace gases play a key role in many different areas. Examples are the composition of the Earth's atmosphere, industrial emissions, industrial process control, ambient and workplace concentrations in view of health issues, agriculture, medical diagnostics and homeland security [1]. Isotopic compositions of trace gases are of particular interest in such diverse fields as ecological $CO_2$ exchange, volcanic emission or medical diagnostics, because the isotope ratio provides additional information about the origin of the trace gas, or can be used for process identification or as tracer. For example, in ecosystem research isotopic ratios of $CO_2$, $H_2O$, $N_2O$, NO and $NO_2$ [2, 3] enable the determination of the source of emission.

✉ Fax: +41-44-633-12-30, E-mail: sigrist@iqe.phys.ethz.ch

As examples, $CO_2$ sources include soil, plants or combustion during energy conversion as a result of anthropogenic activity. In volcanic research isotopic ratios such as $H^{35}Cl/H^{37}Cl$ or $^{13}CO_2/^{12}CO_2$ are important as magmatic gases may react with rocks and other fluids on their path to the Earth's surface. Hence, changes of isotopic ratios in emitted gases can serve as indicators of increased volcanic activity, especially for sensing the progress towards eruption [4, 5]. A further area of isotope selective trace gas monitoring is in non-invasive medical diagnostics [6], e.g. isotope ratios of $CO_2$ have been identified as being indicators for the presence of *Helicobacter pylori*, the bacteria associated with peptic ulcers and gastric cancer [7].

Normally the isotope ratio of a sample is compared to the one of a standard reference gas and the deviation of these ratios is given by the $\delta$-value [8]:

$$\delta = \left( \frac{^{minor}C_{sample}/^{main}C_{sample}}{^{minor}C_{ref}/^{main}C_{ref}} - 1 \right) 1000‰, \tag{1}$$

where $^{main}C$ is the concentration of the main isotopomer and $^{minor}C$ the one of the less abundant isotopomer and the indices sample and ref correspond to sample gas and standard reference gas, respectively.

Today the standard method for such measurements is isotope-ratio mass spectrometry (IRMS). The advantage of IRMS is its high precision and accuracy. As an example, Röckmann et al. [9] developed an IRMS instrument in combination with gas chromatography yielding a reproducibility of ±0.1‰ for $\delta^{15}N$ in $N_2O$. The drawback of IRMS is that it requires careful and time-consuming sample preparation, the instrument is too large for field measurements and allows only a limited number of samples (at best 40 per day) to be analyzed [2, 10]. Another disadvantage of IRMS is that isomers, like $^{14}N^{15}N^{16}O$, $^{15}N^{14}N^{16}O$ and $^{14}N_2{}^{17}O$, cannot be distinguished directly. Therefore, a direct on-site measurement technique, which enables a high frequency of measurements of isotopic ratios with high precision (ideally ±0.1‰), would be a real breakthrough in the field of flux measurements and partitioning. In recent years laser spectroscopy has attracted considerable attention as a useful alternative because it needs no sample preparation, it can potentially be used for field measurements and it offers a good selectivity, especially

regarding isotopomers and isomers, and a good time resolution.

Until now most of the laser spectroscopic measurements of isotope ratios were done with high concentrations; especially, $N_2O$ isotopomers were only measured in pure samples. Uehara et al. [11] measured the $^{15}N/^{14}N$ ratio in pure $N_2O$ with a diode laser at $2\,\mu m$ with a precision of $\Delta\delta = 0.3‰$ in a multipass cell by using two different path lengths for the main and the less abundant isotopomers (balanced path length detection scheme). Gagliardi et al. [12] obtained a precision of $\Delta\delta = 9‰$ in pure $N_2O$ with a quantum cascade laser (QCL) at $8\,\mu m$ in a single-path cell. For the $^{13}C/^{12}C$ ratio of $CO_2$ in atmospheric air the best precision of $\Delta\delta = 0.18‰$ was obtained by McManus et al. [13] with a pulsed QCL at $4.3\,\mu m$ and a multipass cell with balanced path length detection. But, the problem in this case was that the line width of the laser exceeded the line width of the absorption lines.

For many applications the concentrations are, however, rather low. Here we focus on nitrous oxide (laughing gas, $N_2O$), whose concentration in ambient air is typically 300 ppb. Its isotopic composition gives important information, e.g. on ecosystem gas exchange [14]. The atmospheric concentration of $N_2O$ has increased from 270 ppb to 314 ppb in the last 200 years [15]. In the same time the abundance of the heavy isotopes has decreased by $\delta(^{15}N^{14}N^{16}O) = -1.8‰$, $\delta(^{14}N^{15}N^{16}O) = -2.2‰$ and $\delta(^{14}N_2{}^{18}O) = -1.2‰$ [16]. This change in the isotopic signature indicates a change in the global sources of $N_2O$ since the beginning of industrialization. For nitrogen the international standard is the $N_2$ of the atmosphere ($^{15}N/^{14}N = 0.3613 \times 10^{-2}$) [17]. Isotope fractionation of $N_2O$ occurs mostly in the stratosphere by photolytic decomposition, where the lighter isotope is preferred, leading to an enrichment of the heavier isotopes of the stratospheric $N_2O$. In addition, the fractionation of $N_2O$ depends on the position of the N isotope within the linear $N_2O$ isotopomer molecule, i.e. there is a difference according to whether the $^{15}N$ is in the center or at the end of the $N_2O$ molecule [18]. Since this fractionation happens mainly in the stratosphere the isotopic composition of $N_2O$ in the Earth's atmosphere depends strongly on the altitude.

Our project focuses on high-precision measurements of isotope ratios of gases at trace concentration, particularly of $N_2O$ isotopomers at ppm levels. We developed and implemented a mid-infrared laser spectrometer based on difference-frequency generation and two different detection schemes, namely balanced path length detection and single long path detection. The spectra were recorded with two different methods, wavelength modulation (WM) and direct absorption spectroscopy. All combinations of measurement methods and detection schemes were tested regarding precision of a single measurement and long-term stability, and the advantages and disadvantages are discussed.

## 2    Experimental arrangement of laser spectrometer

### 2.1    Difference-frequency generation

The fundamental absorption lines of $N_2O$ isotopomers lie in the $4–5\,\mu m$ wavelength range where tunable laser sources are not as readily available as in the near infrared (IR). The important region between $4\,\mu m$ and $5\,\mu m$ is

accessible by lead salt diode lasers, quantum cascade lasers (QCLs) and systems using nonlinear crystals like difference-frequency generation (DFG) or optical parametric oscillators (OPOs) [19]. Lead salt diode lasers need cryogenic cooling and the mode-hop-free tuning range of these lasers is rather limited. Pulsed QCLs work at room temperature or with thermoelectric cooling, but their frequency chirp often results in a line width larger than the absorption lines of the measured gases at a reduced pressure of 50 mbar, which is required in this experiment to differentiate between isotopomer lines. Continuous-wave (cw) QCLs offer narrow line widths but at present commercially available devices still need cryogenic cooling for wavelengths shorter than $5\,\mu m$. Wavelength tuning of QCLs is done by temperature, resulting in a limited tuning range of a few $cm^{-1}$. First devices operating at room temperature for wavelengths around $4\,\mu m$ have been demonstrated recently and first developments of QCLs with external cavity, offering a larger tuning range of more than $100\,cm^{-1}$, have been reported for longer wavelengths in 2006 [20], but they are not commercially available yet. OPOs offer high power and a large wavelength range but in order to achieve a small line width an etalon must be implemented, leading to a limited mode-hop-free tuning range, especially when working under computer control. As a result, our requirements of broad tunability in the $4–5\,\mu m$ region, narrow line width and room-temperature operation are currently best met with a cw DFG system, yet at the cost of complexity and laser power.

In order to cover the wavelength range around 4 to $5\,\mu m$, to access CO and $CO_2$ in addition to $N_2O$ [21], we built a DFG system with a periodically poled $LiNbO_3$ (PPLN) crystal as nonlinear optical medium. The experimental arrangement of the DFG source is depicted in Fig. 1. It is based on a diode-pumped cw Nd:YAG laser (Innolight Mephisto, 2 W, 1064.5 nm) as signal source and a tunable cw external cavity diode laser (ECDL, Sacher TEC-120-850-150, 120 mW, 820–875 nm) as pump laser. The two laser beams are mixed in an antireflection-coated periodically poled MgO-doped $LiNbO_3$ (MgO:PPLN) crystal (HC Photonics, 50 mm × 6 mm × 0.5 mm). After the crystal the near-IR light is blocked with a germanium filter. This source provides a continuous tuning range from $4.3\,\mu m$ to $4.7\,\mu m$ (idler) by



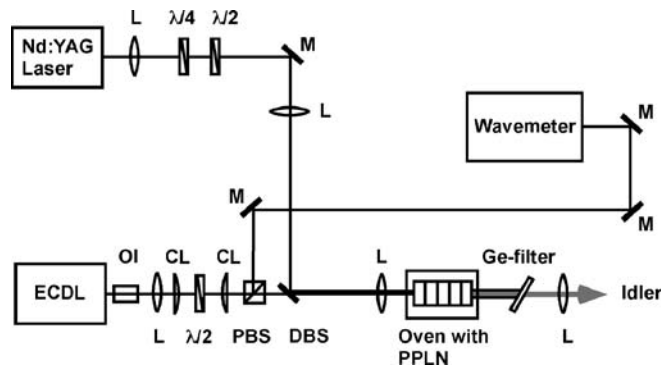**FIGURE 1**    Setup for difference-frequency generation. The beams of a Nd:YAG laser (1064.5 nm, 2 W) and an external cavity diode laser (ECDL, 820–875 nm, 120 mW) are mixed in a periodically poled $LiNbO_3$ (PPLN) crystal, generating light at $4.3–4.7\,\mu m$ of $5–23\,\mu W$ (OI: optical isolator, L: lens, CL: cylindrical lens, $\lambda/2$ and $\lambda/4$: half-wave and quarter-wave plates, M: mirror, PBS: polarizing beam splitter, DBS: dichroic beam splitter)

using only one crystal grating with a period of 23.1 μm, when quasi-phase matching is realized by changing the crystal temperature between 30 °C and 130 °C.

Since LiNbO$_3$ has an absorption band at 5 μm, the power decreases strongly with increasing wavelength. At 4.3 μm the absorption coefficient $\alpha$ of LiNbO$_3$ is 0.25 cm$^{-1}$; at 4.7 μm it amounts to 0.75 cm$^{-1}$ [22]. With a longer crystal length more mid-infrared light is generated but also more is absorbed; therefore, there is an optimal crystal length with the highest conversion efficiency. The idler power $P_i$ is given by the following equation in SI units [23–25]:

$$P_i = P_p P_s \frac{32\pi^2 d_{eff}^2 L}{\varepsilon_0 c n_i \lambda_i^2 \left(n_s \lambda_p + n_p \lambda_s\right)} h\left(\xi, \sigma, \mu, \alpha, L\right) , \tag{2}$$

where $d_{eff}$ is the effective nonlinear coefficient of the PPLN crystal, $L$ is the crystal length, $\varepsilon_0$ is the vacuum permittivity, $c$ is the speed of light, $P$ is the laser power, $\lambda$ is the wavelength and $n$ is the refractive index, with the subscripts p, s and i referring to pump, signal and idler, respectively. The focusing function $h(\xi, \sigma, \mu, \alpha, L)$ for diffraction-limited Gaussian beams is given by

$$h\left(\xi, \sigma, \mu, \alpha, L\right) =$$
$$\mathrm{Re}\left(\frac{e^{-\alpha L/2}}{4\xi} \int_{-\xi}^{\xi} d\tau \int_{-\xi}^{\xi} d\tau' \frac{\exp(-i\sigma(\tau+\tau') + \frac{\alpha L}{4\xi}(\tau-\tau'))}{1 + \tau\tau' - i\frac{1+\mu^2}{1-\mu^2}(\tau-\tau')}\right) , \tag{3}$$

where

$$\xi = \frac{L}{b} , \tag{4}$$

$$\mu = \frac{k_s}{k_p} = \frac{n_s \lambda_p}{n_p \lambda_s} , \tag{5}$$

$$\sigma = -\pi b \left(\frac{n_p}{\lambda_p} - \frac{n_s}{\lambda_s} - \frac{n_i}{\lambda_i} - \frac{1}{\Lambda}\right) . \tag{6}$$

Here $\Lambda$ denotes the grating period of the PPLN crystal and $b$ the confocal parameter of both pump and signal lasers, given by the minimal beam waist $b = k_p \omega_p^2 = k_s \omega_s^2$. Our calculations have shown that the optimal parameters $\xi$ and $\sigma$ depend only slightly on wavelength and are given by $\xi = 1.3$ and $\sigma = 1.3$. The optimal crystal length was calculated to be $L > 10$ cm at 4.3 μm, $L = 5.9$ cm at 4.6 μm and $L = 4.0$ cm at 4.7 μm; therefore, a crystal length of $L = 5.0$ cm was chosen.

The generated idler power was measured with a thermo-electrically cooled detector (VIGO PDI-2TE-5). At 4.3 μm 23 μW were generated, at 4.6 μm 8 μW and at 4.7 μm 5 μW. This is about four to ten times lower than calculated, most probably because of imperfections in the crystal, grating quality and non-Gaussian beam shape of the external cavity diode laser. The line width of the idler is given by a convolution between the line widths of the ECDL (1 MHz) and the Nd:YAG laser (1 kHz). In our case the idler line width is dominated by the ECDL and amounts to 1 MHz. The line width is an important issue for studies of isotopomers, as the absorption lines of the different isotopomers are close to each other and measurements need to be performed at reduced gas pressure to reduce collisional broadening and enable sufficient specificity.

## 2.2   *Absorption cells and experimental arrangement*

One problem in measuring isotopomers is that the concentration of the main isotope is often considerably higher than that of the less abundant isotope (e.g. $^{14}$N$^{15}$N$^{16}$O$/^{14}$N$_2$$^{16}$O = 0.36\%$). There are two possibilities to overcome this problem, either to measure two lines of similar strengths (resulting in a strong temperature sensitivity of the measurement) or by choosing two lines with similar lower energy levels but with very different line strengths (corrected with the natural abundance). The temperature dependence of the isotopic ratio $\Delta\delta/\Delta T$ is proportional to the difference of the ground-state energies $\Delta E$ of the corresponding transitions [26]:

$$\frac{\Delta\delta}{\Delta T} \cong \frac{\Delta E}{kT^2} , \tag{7}$$

where $k$ is the Boltzmann constant, $T$ is the absolute temperature and $\delta$ has been defined in (1) above. For most applications the required precision is $\Delta\delta = 1\%$, or less, so either the gas cell needs to be very well temperature stabilized or a balanced path length setup should be used.

In our setup we use an astigmatic multipass Herriott cell (New Focus 5611), which offers the possibility to enter the cell at two different angles, so that the incident beam either leaves the cell after only two passes or after the usual 182 passes [13]. This yields two different path lengths of 36 m (182 passes) or 40 cm (two passes), respectively. This balanced path length approach enables the measurement of two lines of very different line strengths.

The concentration of the measured gas is given by the area under the absorption line divided by the line intensity. To measure differences in concentrations of less than 1‰, a precise measurement of the wavelength is required and the line intensities should be known exactly. To avoid these problems a reference cell is used to measure a sample gas and the reference gas simultaneously. We designed and built a single-pass cell that offers two different path lengths. It consists of a tube (stainless steel) and antireflection-coated CaF$_2$ windows. No Brewster windows were used to avoid path-length changes if the beam position was shifted slightly. The long path of 50 cm is along the tube and the short path of 1 cm is perpendicular to the tube. This yields a path-length ratio of 1 : 50 compared to 1 : 91 for the multipass cell. The long path of the reference cell could be doubled to 100 cm by having two passes, yielding a path-length ratio of 1 : 100. But, the short path length of 1 cm demands a narrow tube (diameter 6 mm), so for a second pass along the long path the beam would need to be refocused by using a curved mirror making this setup rather complex.

The experimental arrangement is presented in Fig. 2. After the DFG system a beam splitter (CaF$_2$ plate) directs part of the light to the reference cell. The second reflection of the plate is used for the short path in the multipass cell. In front of the reference cell is a second beam splitter to direct a part along the short path through the reference cell. We used InSb detectors with liquid-nitrogen cooling (Judson Technologies J10D-M204-R04M-60) with an active area of $4 \times 4$ mm$^2$ for recording the beam power.
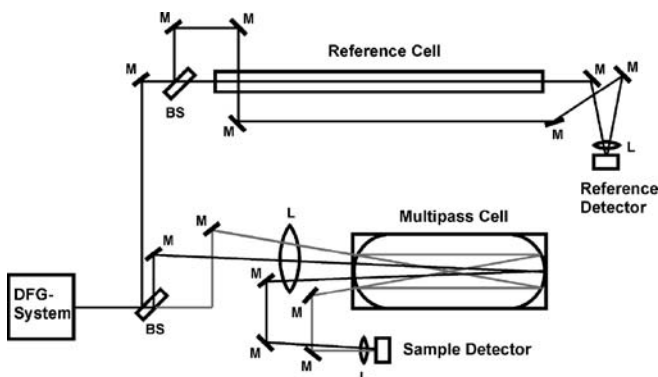
**FIGURE 2** Setup for the balanced path length detection scheme consisting of an astigmatic Herriott cell and a single-pass reference cell. If the beam enters the multipass cell at a small angle, the beam leaves the cell after only two passes (40 cm) instead of 182 (36 m). Also, the reference cell has two different path lengths, along the tube (50 cm) and perpendicular to the tube (1 cm) (BS: beam splitter (CaF$_2$ plate), M: mirror, L: lens)

## 3    Measurements

### 3.1    Methods

Two different measurement methods were tested, wavelength modulation (WM) with first-harmonic detection and direct absorption spectroscopy. For wavelength modulation the wavelength of the ECDL was modulated across the absorption line with a frequency of 1 kHz and a modulation index of 2. The detector signals were recorded with lock-in amplifiers (Stanford Research Systems, SR830 DSP) with a time constant of 100 ms for long-path measurements and 300 ms for short-path measurements. A measurement of all three N$_2$O isotopomers ($^{14}$N$^{15}$N$^{16}$O, $^{15}$N$^{14}$N$^{16}$O, $^{14}$N$_2$$^{16}$O) takes about 30 min. The measured spectrum is similar to the derivative of the absorption line. The advantage of WM is its zero background, i.e. no signal without absorption. But, any wavelength-dependent change of laser power produces a signal at the detector, e.g. interference fringes caused by optical elements result in a wavelength-dependent background.

For direct absorption spectroscopy the wavelength was scanned across the absorption lines of all three isotopomers and the detector signal was recorded by a data-acquisition card (DAQ, CompuScope14100, 14-bit resolution, 100 MS/s). The scans were performed by applying a sinusoidal voltage at 500 Hz to the piezo of the ECDL. To improve the signal to noise ratio 1000 scans were averaged for long-path measurements and 5000 scans for short-path measurements. From these measurements a moving average over 21 points was taken. For 200 averaged scans it takes 15 min for single long path and 1.5 h for balanced path length detection.

### 3.2    Absorption line selection and sample preparation

For the selection of the absorption lines several important points must be considered. First, the lines should be free of interference with other isotopomers or other molecules. Second, the line strength, corrected with the natural abundance, should be similar for all isotopomers if using the single long path detection scheme, or the lower energy level should be similar for all three isotopomers if using the balanced path length detection scheme to reduce the tempera-

ture dependence of the measurement (see (7)). And, finally, the positions of the lines should be within the wavelength range covered by the piezo scan of the ECDL. The chosen absorption lines are at 2188.6876 cm$^{-1}$ ($^{14}$N$^{15}$N$^{16}$O), 2188.7560 cm$^{-1}$ ($^{15}$N$^{14}$N$^{16}$O), 2188.9384 cm$^{-1}$ ($^{14}$N$_2$$^{16}$O, weak line) and 2188.1894 cm$^{-1}$ ($^{14}$N$_2$$^{16}$O, strong line) [27]. These lines fulfill the above requirements, with the only exception of the lower energy level $E_{low}$ of the strong line ($E_{low} = 588.8$ cm$^{-1}$) of the main isotope, which is not as close to the lower energy levels of the other isotopomers ($^{14}$N$^{15}$N$^{16}$O: $E_{low} = 76.2$ cm$^{-1}$ and $^{15}$N$^{14}$N$^{16}$O: $E_{low} = 97.2$ cm$^{-1}$) as it could be, but it is still better than the weak line of the main isotopomer $^{14}$N$_2$$^{16}$O ($E_{low} = 1198.4$ cm$^{-1}$). The absorption line of $^{14}$N$_2$$^{16}$O at 2211.3982 cm$^{-1}$ would fit better (lower energy level at $E_{low} = 87.98$ cm$^{-1}$) but it was outside the piezo scan range of the ECDL and therefore could not be reached under computer control.

The measurements were made at room temperature and at a total gas pressure of 50 mbar to avoid overlapping of the absorption lines. The N$_2$O concentration in the reference cell was 5% from a certified mixture. The concentration in the sample cell was either 825 ppm, obtained by diluting the gas from the 5% mixture with room air (8.0 mbar 5% N$_2$O mixed with room air to 900 mbar) or 100 ppm from another certified mixture. The concentration of the mixture with room air is about two times higher than expected because of adsorption and desorption effects of the N$_2$O molecules to the cell walls during the diluting process. Experiments were done with wavelength modulation as well as with direct absorption spectroscopy in combination with balanced path length detection or single long path detection. All four versions were tested and the results are compared regarding both the precision of a single measurement and the long-term stability.

### 3.3    Data evaluation

At low concentrations the detector signal measured with wavelength modulation is proportional to the concentration of the gas [28]. Therefore, the $\delta$-value (1) can be obtained by taking the ratio of the measured signals of the sample and the reference gas for both isotopomers and by comparing these ratios for the absorption lines of the main and the less abundant isotopomers.

To evaluate the data from our measurements we did not take the ratios mentioned above directly but plotted the detector signal $^I S_{sample}(\tilde{\nu})$ at frequency $\tilde{\nu}$ recorded after the sample gas cell versus the detector signal $^I S_{ref}(\tilde{\nu})$ recorded after the reference cell, for the isotopomer $I$. The fitted curve is a linear relation between sample signal and reference signal. A second-order baseline is added to take a background (fringes caused by windows, etc.) into account:

$$^I S_{sample}(\tilde{\nu}) = {}^I a \, {}^I S_{ref}(\tilde{\nu}) + b_0 + b_1 \tilde{\nu} + b_2 \tilde{\nu}^2 . \tag{8}$$

By repeating this procedure for each isotopomer $I$ and comparing the slopes $^I a$ of these curves of the main and the less abundant isotopomers, the difference of the isotopic composition between the sample gas and the reference gas can be calculated [28]:

$$\delta = \left( \frac{^{minor}C_{sample}/^{main}C_{sample}}{^{minor}C_{ref}/^{main}C_{ref}} - 1 \right) 1000‰$$

$$= \left( \frac{{}^{minor}C_{sample}/{}^{minor}C_{ref}}{{}^{main}C_{sample}/{}^{main}C_{ref}} - 1 \right) 1000\%o$$

$$\delta = \left( \frac{{}^{minor}ratio}{{}^{main}ratio} - 1 \right) 1000\%o = \left( \frac{{}^{minor}a}{{}^{main}a} - 1 \right) 1000\%o. \quad (9)$$

Here ${}^{main}C_{ref,sample}$ and ${}^{minor}C_{ref,sample}$ are the concentrations of the main and the less abundant (minor) isotopomers of the reference gas and the sample gas, respectively, and the ratios are given by ${}^{main}ratio = {}^{main}C_{sample}/{}^{main}C_{ref}$ and ${}^{minor}ratio = {}^{minor}C_{sample}/{}^{minor}C_{ref}$. The advantage of this method is that there is no need for correcting constant backgrounds. Figure 3 shows the result for wavelength modulation with single long path detection.

The measurements with the data-acquisition card were evaluated similarly. A baseline was obtained by fitting the part between the absorption lines with a polynomial of tenth order. This baseline was subtracted and the detector signal of each absorption line was plotted versus the detector signal of the corresponding reference absorption line. Then, the slope was determined as described in (8) for each isotopomer and the $\delta$-value was calculated by comparing the slopes.

## 4        Results and discussion

Wavelength modulation in combination with single long path detection yields the best precision for a single measurement (3‰) and good reproducibility (6‰) as long as the temperature of the gas is stable. The influence of a temperature change can be seen in Fig. 4a when the sample gas was accidentally cooled when refilling the detector with liquid nitrogen standing next to the sample cell. With the measurements during the temperature change included, the reproducibility is 18‰ for $\delta({}^{14}N^{15}N^{16}O/{}^{15}N^{14}N^{16}O)$ and $\delta({}^{15}N^{14}N^{16}O/{}^{14}N_2{}^{16}O)$. However, $\delta({}^{14}N^{15}N^{16}O/{}^{15}N^{14}N^{16}O)$ is not influenced by the temperature change, because the ratio
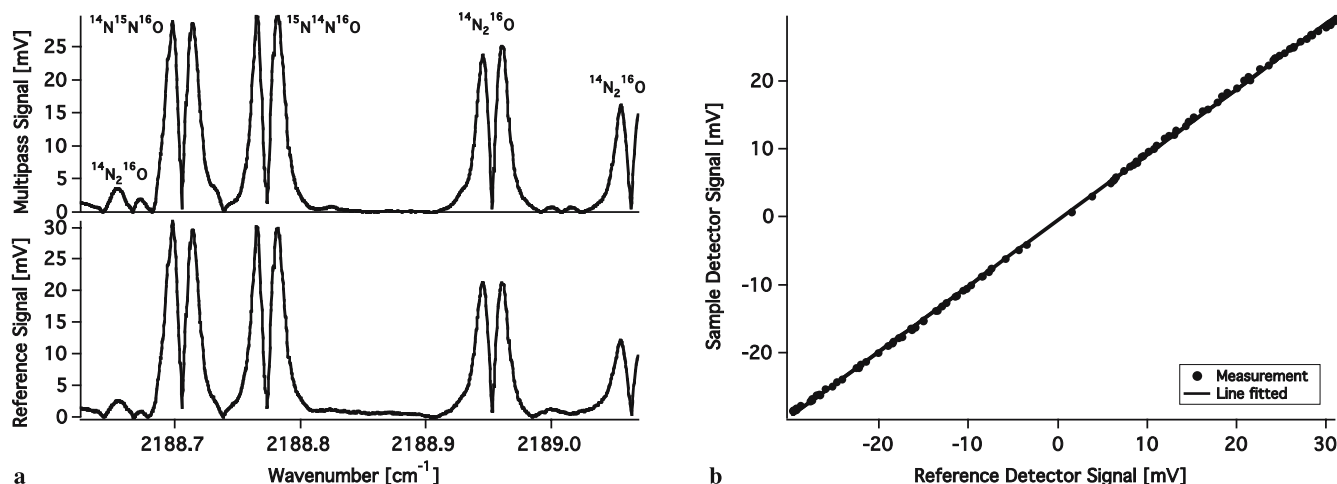


**FIGURE 3**   (**a**) Absorption lines of $N_2O$ isotopomers measured with wavelength modulation (WM) and single long path detection. (**b**) The WM measurements are evaluated by plotting the detector signal from the sample versus the detector signal from the reference gas, here shown for ${}^{14}N^{15}N^{16}O$. By comparing the slopes of these lines of each isotopomer, the $\delta$-values can be calculated
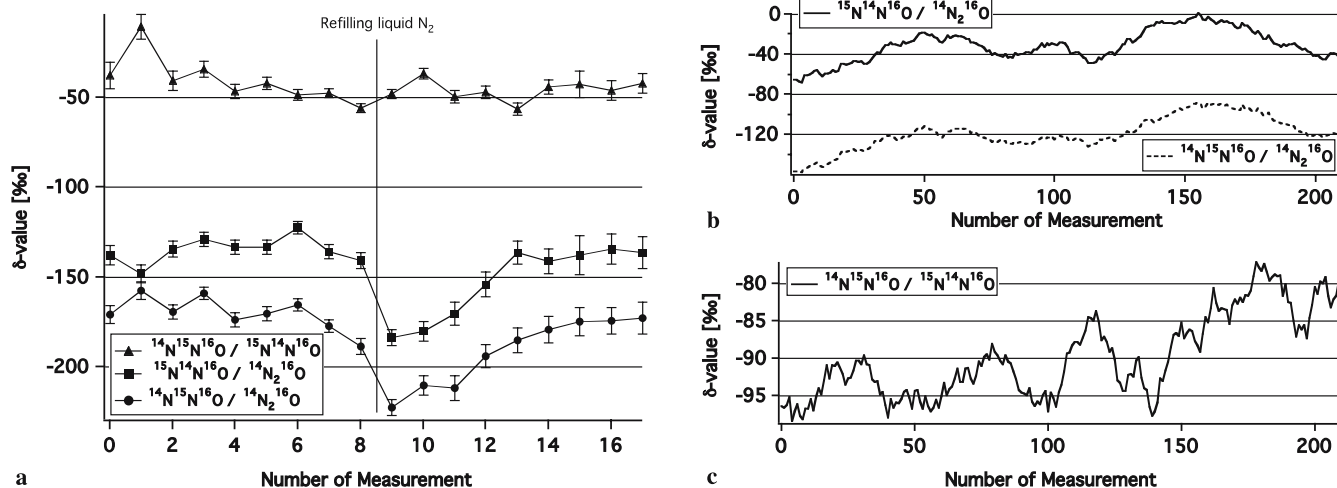


**FIGURE 4**   (**a**) $\delta$-value for different isotopomers of $N_2O$ measured with wavelength modulation combined with single long path detection. There is a strong change in $\delta({}^{15}N^{14}N^{16}O/{}^{14}N^{14}N_2{}^{16}O)$ and $\delta({}^{14}N^{15}N^{16}O/{}^{14}N_2{}^{16}O)$ when the temperature of the sample gas changed because of refilling the detector with liquid nitrogen standing next to the cell. $\delta({}^{14}N^{15}N^{16}O/{}^{15}N^{14}N^{16}O)$ did not change because it is nearly temperature independent. (**b**) The same isotopomers measured with the data-acquisition card. Also, here the temperature dependence of $\delta({}^{14}N^{15}N^{16}O/{}^{14}N_2{}^{16}O)$ and $\delta({}^{15}N^{14}N^{16}O/{}^{14}N_2{}^{16}O)$ can be observed. (**c**) The stability of $\delta({}^{14}N^{15}N^{16}O/{}^{15}N^{14}N^{16}O)$ is higher because this ratio is less temperature dependent

| Method | Concentration | Isotope ratios | δ-value average | Precision of a single measurement | Reproducibility | Number of measurements |
|---|---|---|---|---|---|---|
| WM | 825 ppm sample | $\dfrac{^{14}N^{15}N^{16}O}{^{14}N_2{}^{16}O}$ | −184‰ | 3.3‰ | 8.6‰ with temperature change: 18‰ | 19 |
| single long path | | $\dfrac{^{15}N^{14}N^{16}O}{^{14}N_2{}^{16}O}$ | −145‰ | 3.5‰ | 5.9‰ with temperature change: 18‰ | |
| | 5% reference | $\dfrac{^{14}N^{15}N^{16}O}{^{15}N^{14}N^{16}O}$ | −45.9‰ | 2.3‰ | 6.0‰ | |
| WM | 100 ppm sample | $\dfrac{^{14}N^{15}N^{16}O}{^{14}N_2{}^{16}O}$ | 49.4‰ | 4.8‰ | 6.4‰ | 10 |
| single long path | | $\dfrac{^{15}N^{14}N^{16}O}{^{14}N_2{}^{16}O}$ | 80.5‰ | 5.3‰ | 6.9‰ | |
| old reference cell (10-cm long) | 5% reference | $\dfrac{^{14}N^{15}N^{16}O}{^{15}N^{14}N^{16}O}$ | −28.8‰ | 4.1‰ | 6.6‰ | |
| WM | 825 ppm sample | $\dfrac{^{14}N^{15}N^{16}O}{^{14}N_2{}^{16}O}$ | 230‰ | 11‰ | 17‰ | 10 |
| balanced path length | | $\dfrac{^{15}N^{14}N^{16}O}{^{14}N_2{}^{16}O}$ | 274‰ | 12‰ | 14‰ | |
| | 5% reference | $\dfrac{^{14}N^{15}N^{16}O}{^{15}N^{14}N^{16}O}$ | −35.2‰ | 10‰ | 10‰ | |
| DAQ | 825 ppm sample | $\dfrac{^{14}N^{15}N^{16}O}{^{14}N_2{}^{16}O}$ | −119‰ | 4.5‰ | 16‰ | 210 |
| single long path | | $\dfrac{^{15}N^{14}N^{16}O}{^{14}N_2{}^{16}O}$ | −31.5‰ | 5.0‰ | 15‰ | |
| | 5% reference | $\dfrac{^{14}N^{15}N^{16}O}{^{15}N^{14}N^{16}O}$ | −89.9‰ | 3.8‰ | 5.6‰ | |
| DAQ | 825 ppm sample | $\dfrac{^{14}N^{15}N^{16}O}{^{14}N_2{}^{16}O}$ | 145‰ | 6.4‰ | 11‰ | 203 |
| balanced path length | | $\dfrac{^{15}N^{14}N^{16}O}{^{14}N_2{}^{16}O}$ | 172‰ | 6.3‰ | 9.5‰ | |
| | 5% reference | $\dfrac{^{14}N^{15}N^{16}O}{^{15}N^{14}N^{16}O}$ | −22.7‰ | 5.6‰ | 12‰ | |

**TABLE 1**    Results of isotope ratio measurements for $N_2O$ isotopomers obtained with different measurement techniques combined with balanced path length or single long path detection schemes for different concentrations (WM: wavelength modulation, DAQ: data-acquisition card; for definition of δ see (1))

of the absorption line strengths involved is nearly temperature independent in this case. In addition to the temperature dependence, a further disadvantage of this method is that it takes about 30 min to record one spectrum, leading to a low time resolution.

Wavelength modulation combined with balanced path length detection is less temperature dependent than single long path measurements. But, it yields a worse precision of a single measurement (12‰) and accordingly a reproducibility of 14‰, which is still better than before with single long path detection. The precision, though, is worse than before because only a small part of the light is directed along the short path, yielding a worse signal to noise ratio on the detector. Again, the recording of a spectrum takes 30 min. Direct absorption spectroscopy measured with the data-acquisition card in combination with the single long path detection scheme yields a good precision of a single measurement (5‰), but the reproducibility (15‰) is worse than the precision because of the temperature dependence of this method as seen in Fig. 4b. The reproducibility of the $^{14}N^{15}N^{16}O/^{15}N^{14}N^{16}O$ ratio is 6‰, because it is much less

temperature dependent (see Fig. 4c). The advantage of this method is its improved time resolution; it takes only 15 min for 200 measurements.

When the spectrum is recorded with the data-acquisition card in combination with the balanced path length detection scheme the reproducibility is improved (10‰). The precision (6‰) is better than the reproducibility, but it is worse than with single long path detection because of the worse signal to noise ratio for the short path. The low laser power along the short path also requires more averaging of scans, resulting in a lower time resolution. It takes 90 min for 200 measurements, which is still much better than when using wavelength modulation. All the results are listed in Table 1.

When the same gas, though at different concentrations, is filled in the reference cell and the multipass cell the δ-value is expected to be zero. But, our measurements yield an offset depending on the measurement method and path-length ratios (Table 1). Such an offset has also been observed by other authors [28–30]. It may be explained by path-length ratios not known precisely enough, by pressure or temperature differences between sample and reference gases or by nonlinearities

| Method | Advantage | Disadvantage |
|---|---|---|
| WM and single long path | + Signal to noise ratio | – Temperature dependence<br>– Time resolution |
| WM and balanced path lengths | + Temperature dependence | – Time resolution<br>– Signal to noise ratio |
| DAQ and single long path | + Time resolution<br>+ Signal to noise ratio | – Temperature dependence |
| DAQ and balanced path lengths | + Time resolution<br>+ Temperature dependence | – Signal to noise ratio |

**TABLE 2**   Advantages and disadvantages of different measurement methods in combination with different detection schemes (WM: wavelength modulation, DAQ: data-acquisition card)

in the detector response. When the day-to-day reproducibility is good enough this offset can be measured once and then subtracted for subsequent measurements. For measurements with wavelength modulation it also needs to be considered that (9) is only valid for small absorption; for stronger absorption this equation must be corrected, otherwise the evaluation produces an offset [31].

When comparing the different methods it can be concluded that recording the spectrum with the data-acquisition card in combination with balanced path length detection is the most promising method because of its good time resolution and low temperature dependence (Table 2). But, the best results are obtained with wavelength modulation in combination with the single long path detection scheme because of the best signal to noise ratio (Table 1). The main advantages and drawbacks of the four schemes employed are summarized in Table 2.

A reason for the bad reproducibility might be the degradation of the ECDL, whose side-mode suppression was not sufficient any more, yielding additional noise to the measurement. An indication for this is that previous measurements of lower concentrations (100 ppm) have about the same precision and the same reproducibility as the more recent measurements with eight times higher concentrations (Table 1). These measurements were repeated later and gave worse results than originally. Another problem might be the detectors because, depending on the quality of the vacuum, an ice layer is built up on the surfaces of the nitrogen-cooled detectors and their windows. This layer changes the transmission of the light to the detector because ice absorbs in the mid IR and the layer acts as a dielectric coating changing the reflectivity of the window and the detector. Variation of the thickness of this ice layer may cause variations in the measurements, in this way reducing the reproducibility. To reduce this problem the detectors should be evacuated regularly [32].

## 5   Conclusion and outlook

For the first time the isotopic composition of $N_2O$ at trace gas level was measured with laser spectroscopy. A continuously tunable room-temperature laser source based on difference-frequency generation with a periodically poled $LiNbO_3$ crystal was developed for the 4.3–4.7 μm range. This cw laser source has a line width of 1 MHz and yields powers up to 23 μW. Two different measurement methods, wavelength modulation and direct absorption spectroscopy, were tested in combination with two different detection schemes, balanced path length and single long path detection. On the one hand, direct absorption spectroscopy with balanced path

length detection was the most promising method owing to its low temperature sensitivity and its good time resolution, but its precision was not sufficient. On the other hand, wavelength modulation with single long path detection yielded a good precision (3‰) and a good reproducibility (6‰), but was strongly temperature dependent and needed a long measurement time.

There are two main problems, which currently limit the precision and reproducibility. The first is related to the external cavity diode laser (ECDL) whose side-mode suppression was not sufficient any more. This caused sudden mode hops and deteriorated the reproducibility of the measurements.

The second problem is related to the low signal to noise ratio of the detector signals, which is related to the low laser power available. Hence, the precision and reproducibility could be substantially improved by higher laser powers, preferentially in the mW range, and stable laser emission. Future near-room-temperature cw QCLs around 4.6 μm with broader tunability appear very promising. Another possibility would be DFG with a waveguide nonlinear crystal, offering a much higher conversion efficiency because of better confinement of the laser beams, once they become commercially available for the needed wavelengths.

## REFERENCES

1  F.K. Tittel, A.A. Kosterev (guest eds.), Appl. Phys. B **85**, 171 (2006)
2  D. Yakir, L.S.L. Sternberg, Oecologia (Berlin) **123**, 297 (2000)
3  D.R. Bowling, S.D. Sargent, B.D. Tanner, J.R. Ehleringer, Agric. For. Meteorol. **118**, 1 (2003)
4  T. Tesdesco, P. Sarsi, Earth Planet. Sci. Lett. **171**, 465 (1999)
5  F.K. Tittel, D. Weidmann, C. Oppenheimer, L. Gianfrani, Opt. Photon. News **17**, 24 (2006)
6  A. Amann, D. Smith (eds.), *Breath Analysis for Clinical Diagnosis and Therapeutic Monitoring* (World Scientific, Singapore, 2005)
7  S. Koletzko, M. Haisch, I. Seeboth, B. Braden, K. Hengels, B. Koletzko, P. Hering, Lancet **345**, 961 (1995)
8  H. Graig, Geochim. Cosmochim. Acta **12**, 133 (1957)
9  T. Röckmann, J. Kaiser, C.A.M. Brenninkmeijer, W. Brand, Rapid Commun. Mass Spectrom. **17**, 1897 (2003)
10  D.R. Bowling, P.P. Tans, K.M. Russel, Global Change Biol. **7**, 127 (2001)
11  K. Uehara, K. Yamamoto, T. Kikugawa, N. Yoshida, Spectrochim. Acta A **59**, 957 (2003)
12  G. Gagliardi, S. Borri, F. Tamassia, F. Capasso, C. Gmachl, D.L. Sivco, J.N. Baillargeon, A.L. Hutchinson, A.Y. Cho, Isotopes Environ. Health Stud. **41**, 313 (2005)
13  J.B. McManus, D.D. Nelson, J.H. Shorter, R. Jimenez, S. Herndon, S. Saleska, M. Zahniser, J. Mod. Opt. **52**, 2309 (2005)
14  D. Yakir, X.F. Wang, Nature **380**, 515 (1996)
15  T. Rahn, M. Wahlen, Science **278**, 1776 (1997)

16 T. Röckmann, J. Kaiser, C.A.M. Brenninkmeijer, Atmosph. Chem. Phys. **3**, 315 (2003)

17 W.M. White, *Geochemistry* (John-Hopkins University Press, Cornell, 1997), Online Textbook, Chapt. 9 [www.geo.cornell.edu/geology/classes/geo455/Chapters.html]

18 T. Röckmann, J. Kaiser, C.A.M. Brenninkmeijer, J.N. Crowley, R. Borchers, W.A. Brand, P.J. Crutzen, J. Geophys. Res. **106**, 10 403 (2001)

19 I.T. Sorokina, K.L. Vodopyanov (eds.), *Solid-State Mid-Infrared Laser Sources* (Top. Appl. Phys. **89**) (Springer, Berlin Heidelberg, 2003)

20 J. Faist, Opt. Photon. News **17**, 32 (2006)

21 H. Waechter, M.W. Sigrist, Mid-infrared coherent sources and applications, in *Mathematics, Physics and Chemistry* (Nato Sci. Ser. II), ed. by M. Ebrahimzadeh, I.T. Sorokina (Springer, Berlin Heidelberg, 2006)

22 L.E. Myers, R.C. Eckhardt, M.M. Feyer, R.L. Byer, W.R. Bosenberg, Opt. Lett. **21**, 591 (1996)

23 S. Borri, P. Cancio, P. De Natale, G. Giusfredi, D. Mazzotti, F. Tamassia, Appl. Phys. B **76**, 473 (2003)

24 G.D. Boyd, D.A. Kleinman, J. Appl. Phys. **36**, 3597 (1968)

25 T.B. Chu, M. Broyer, J. Phys. France **45**, 1599 (1984)

26 P. Bergamaschi, M. Schupp, G.W. Harris, Appl. Opt. **33**, 7704 (1994)

27 L.S. Rothman, D. Jacquemart, A. Barbe, D.C. Benner, M. Birk, L.R. Brown, M.R. Carleer, C. Chackerian Jr., K. Chance, L.H. Coudert, V. Dana, V.M. Devi, J.-M. Flaud, R.R. Gamache, A. Goldman, J.-M. Hartmann, K.W. Jucks, A.G. Macki, J.-Y. Mandin, S.T. Massie, J. Orphal, A. Perrin, C.P. Rinsland, M.A.H. Smith, R.N. Tolchenov, R.A. Toth, J. Vander Auwera, P. Varanasi, G. Wagner, J. Quantum Spectrosc. Radiat. Transf. **96**, 139 (2005)

28 G. Gagliardi, A. Castrillo, R.Q. Iannone, E.R.T. Kerstel, L. Gianfrani, Appl. Phys. B **77**, 119 (2003)

29 M. Erdélyi, D. Richter, F.K. Tittel, Appl. Phys. B **75**, 289 (2002)

30 E.R.T. Kerstel, R. van Trigt, N. Dam, J. Reuss, H.A.J. Meijer, Anal. Chem. **71**, 5297 (1999)

31 A. Castrillo, G. Casa, E. Kerstel, L. Gianfrani, Appl. Phys. B **81**, 863 (2005)

32 E. Theocharous, Infrared Phys. Technol. **48**, 175 (2006)